UNIVERSIDAD DE MÁLAGA

ESCUELA TÉCNICA SUPERIOR DE INGENIEROS INDUSTRIALES

ANDALUCÍA TECH
Campus de Excelencia Internacional

Grupo de Mecánica de Fluidos de Málaga

Effect of the axial jet on the optimal response in Batchelor vortex

F. J. Blanco-Rodríguez, J. Hermenegildo García-Ortíz, L. Parras and C. del Pino

Universidad de Málaga, Andalucía Tech, E.T.S. Ingeniería Industrial, C/ Doctor Ortíz Ramos, s/n, 29071 Málaga, SPAIN

Introduction

Wing-tip vortices are circular patterns of rotating air left behind a wing as it generates lift.

Instabilities:

Non-modal stability analysis $(t\sim 0)$
- Response to initial conditions (Optimal perturbation)
  - Transient growth (Mao2012)
- Response to external forcing (**Optimal response**)
  - Time-harmonic forcing (Guo2011)
  - Stochastic forcing (Fontane2008)

Normal mode stability analysis $(t\sim\infty)$
- Strong inviscid helical instability (Heaton2007)
- Weak viscous instabilities (Khorrami1991)
- Weak viscous centre instabilities (Fabre2004)
- Cooperative instability (Hattori2009)

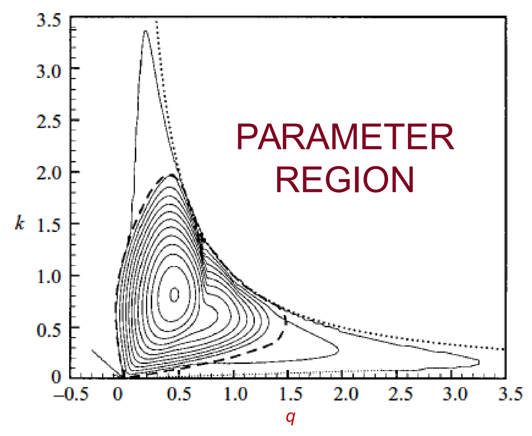

Applications: **Aeronautics:** Optimization of airport traffic decreasing the current spacing between aicrafts in complete safety

Wind energy: Increase the performance in wind farms of turbines since the funcionality of one rotor depends on the incident flow given by the precedent one

Objective: Characterize numerically the response of a time-harmonically force in LNS with a Batchelor vortex as a base flow

Why?

Because the Batchelor vortex is widely adopted in aeronautics

→ Study the effect of swirl parameter q on the optimal response

THUS → Numerical validation (DNS) of the theoretical response and flow structures using a spectral Fourier-based numerical method

[Mao2012] X. Mao and S.J. Sherwin, **697**, *J. Fluid Mech.*, (2012)
[Heaton2007] C. J. Heaton, **576**, *J. Fluid Mech.*, (2007)
[Guo2011] Z.-W Guo and D.-J. Sun, **375**, *Phys. Letters A*, (2011)
[Khorrami1991] M.R. Khorrami, **225**, *J. Fluid Mech.*, (1991)
[Hattori2009] Y. Hattori and Y. Fukumoto, **21**, *Phys. Fluids*, (2009)
[Fontane2008] Fontane et al. , **613**, *J. Fluid Mech.*, (2008)
[Fabre2004] D. Fabre and L. Jacquin, **500**, *J. Fluid Mech.*, (2004)

Governing equations. Stability analysis

Incompressible forced Navier-Stokes equations $\boldsymbol{u}=u(r,\theta,z,t)\boldsymbol{e}_r+v(r,\theta,z,t)\boldsymbol{e}_\theta+w(r,\theta,z,t)\boldsymbol{e}_z$

$$\partial_t\boldsymbol{u}=-(\boldsymbol{u}\cdot\nabla)\boldsymbol{u}-\nabla p+\frac{1}{Re}\nabla^2\boldsymbol{u}+\boldsymbol{f}\,e^{i\omega t},\qquad \nabla\cdot\boldsymbol{u}=0$$

Dimensionless Batchelor base flow $\boldsymbol{U}=U(r,\theta,z,t)\boldsymbol{e}_r+V(r,\theta,z,t)\boldsymbol{e}_\theta+W(r,\theta,z,t)\boldsymbol{e}_z$

$$U(r,\theta,z,t)=0$$
$$V(r,\theta,z,t)=\frac{1}{r}\left(1-e^{-r^2}\right),\quad\Rightarrow\quad \omega_z(r,\theta,z,t)=2e^{-r^2}$$
$$W(r,\theta,z,t)=q^{-1}e^{-r^2}$$

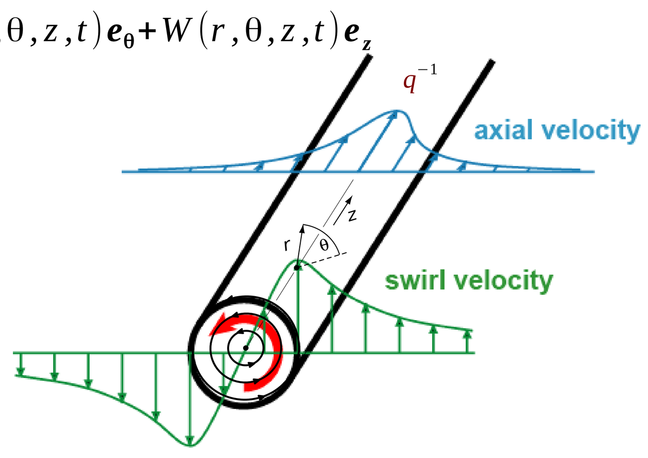

Linearized Navier-Stokes equations $\boldsymbol{u}=\boldsymbol{U}+\boldsymbol{u}'$

$$\partial_t\boldsymbol{u}'=-(\boldsymbol{U}\cdot\nabla)\boldsymbol{u}'-(\boldsymbol{u}'\cdot\nabla)\boldsymbol{U}-\nabla p'+\frac{1}{Re}\nabla^2\boldsymbol{u}'+\boldsymbol{f}\,e^{i\omega t},\qquad \nabla\cdot\boldsymbol{u}'=0$$

Perturbation ansatz

$$(\boldsymbol{u}',p')=(u',v',w',p')=[u'(r,t),v'(r,t),w'(r,t),p'(r,t)]e^{ikz+in\theta}$$
$$k\in\mathbb{R},\quad n\in\mathbb{N}$$

Optimal response analysis

Evolution equation $\boldsymbol{\delta}=[u'(r,t),v'(r,t)]$

$$\partial_t[L]\boldsymbol{\delta}=\left([M]+\frac{1}{Re}[N]\right)\boldsymbol{\delta}+[H]^A\boldsymbol{f}\,e^{i\omega t},\qquad \boldsymbol{u}'=[H]\boldsymbol{\delta},\qquad [H]=\begin{bmatrix}1 & 0\\ 0 & 1\\ \frac{i}{k}\left(\frac{d}{dr}+\frac{1}{r}\right) & -m\frac{k}{r}\end{bmatrix}$$
$$\boldsymbol{\delta}(t=0)=\boldsymbol{\delta}_0$$

$$\partial_t\boldsymbol{\delta}=[A]\boldsymbol{\delta}+[B]\boldsymbol{f}\,e^{i\omega t},\qquad \text{Eigenvalue decomposition}\quad \boldsymbol{\delta}\sim e^{\lambda t}$$
$$\boldsymbol{\delta}(t=0)=\boldsymbol{\delta}_0\qquad [A]=[Q][\lambda][Q]^{-1},\quad \Re(\lambda)<0\ \Rightarrow\ Normal-mode\ STABLE$$

General solution

$$\boldsymbol{u}'_{out}=[H](\boldsymbol{\delta}_h+\boldsymbol{\delta}_p)=[H][Q]e^{[\lambda]t}[Q]^{-1}\boldsymbol{\delta}_0+[H][Q](i\omega-[\lambda])^{-1}[Q]^{-1}[B]\boldsymbol{f}\,e^{i\omega t}$$

Based-kinetic energy norm

Cholesky decomposition

$$2E=\|\boldsymbol{\delta}\|_e^2=\int_0^\infty\left(u'^2+v'^2+w'^2\right)r\,dr\approx\boldsymbol{u}'^A[W]\boldsymbol{u}'=\|[M]\boldsymbol{u}'\|_2^2\quad\Leftrightarrow\quad [W]=[M]^A[M]$$

Optimal response

$$R(\omega)=\max_{f}\frac{\|\boldsymbol{u}'_{out}\|_e^2}{\|\boldsymbol{f}\,e^{i\omega t}\|_e^2}=\max_{f}\frac{\|[H](i\omega-[A])^{-1}[B]\boldsymbol{f}\,e^{i\omega t}\|_e^2}{\|\boldsymbol{f}\,e^{i\omega t}\|_e^2}=\|[H](i\omega-[A])^{-1}[B]\|_e^2$$

Singular value decomposition

$$R(\omega;Re,q,m,k)=\|[M]^{-1}[H](i\omega-[A])^{-1}[B][M]\|_2^2=\|[P]\|_2^2,\qquad R_{max}(\hat{\omega};Re,q,n,k)=s_1$$

$$[P][V]=[S][U]\ \Rightarrow\ [P]\boldsymbol{v}_1=s_1\boldsymbol{u}_1,\qquad \boldsymbol{f}=[M]^{-1}\boldsymbol{v}_1,\quad \boldsymbol{u}'_{out}=[M]^{-1}\boldsymbol{u}_1$$

DNS

Base flow in cartesian coordinates $\boldsymbol{U}=U_x(x,y,z,t)\boldsymbol{e}_x+U_y(x,y,z,t)\boldsymbol{e}_y+U_z(x,y,z,t)\boldsymbol{e}_z$

$$U_x(x,y,z,t)=-\frac{y}{\sqrt{x^2+y^2}}V(x,y,z,t),\quad U_y(x,y,z,t)=\frac{x}{\sqrt{x^2+y^2}}V(x,y,z,t),\quad U_z(x,y,z,t)=q^{-1}e^{-(x^2+y^2)}$$

Fourier spectral method $\boldsymbol{k}=k_x\boldsymbol{e}_x+k_y\boldsymbol{e}_y+k_z\boldsymbol{e}_z$

$$\boldsymbol{u}(x,y,k_z,t)=\iint\hat{\boldsymbol{u}}(k_x,k_y,k_z,t)\;e^{i(k_x x+k_y y)}dk_x\,dk_y$$

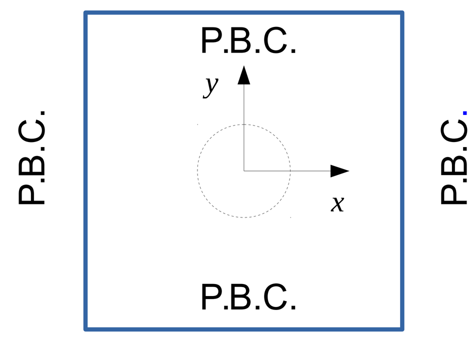

Adams-Bashforth time-integration scheme (Delbende1998)

$$\hat{\boldsymbol{u}}^{n+1}=e^{\frac{k^2\delta t}{Re}}\hat{\boldsymbol{u}}^n+\frac{\delta t}{2}\left(3e^{\frac{k^2\delta t}{Re}}\boldsymbol{N}(\boldsymbol{u}^n,\boldsymbol{f}^n,S_{fringe})+e^{\frac{2k^2\delta t}{Re}}\boldsymbol{N}(\boldsymbol{u}^{n-1},\boldsymbol{f}^{n-1},S_{fringe})\right)$$

Fringe region (Nordström1999)

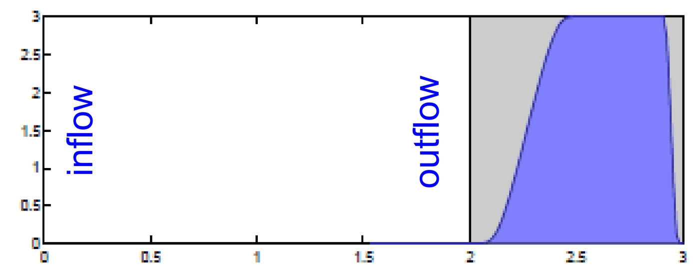

$$S_{fringe}(r)=S_{max}\left[S\left(\frac{r-r_{start}}{\delta_{rise}}\right)-S\left(\frac{r-r_{end}}{\delta_{fall}}\right)\right],$$

$$S(r)=\begin{cases}0 & r\leqslant 0\\ \left(1+e^{\frac{1}{r(r-1)}}\right)^{-1} & 0<r<1\\ 1 & r\geq 1\end{cases}$$

[Delbende1998] I. Delbende et al., **355**, *J. Fluid Mech.*, (1998)
[Nordström1999] J. Nordström et al., **20**, *SIAM J. Sci. Comput.*, (1999)

Results

Lamb-Oseen vortex $n=1$

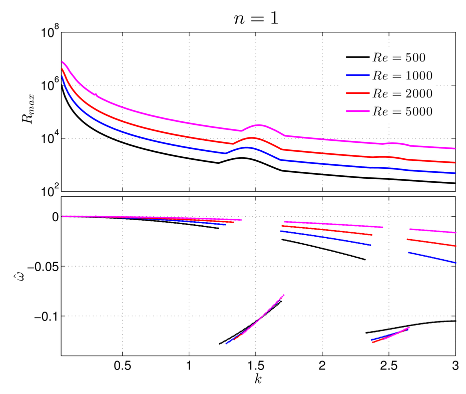

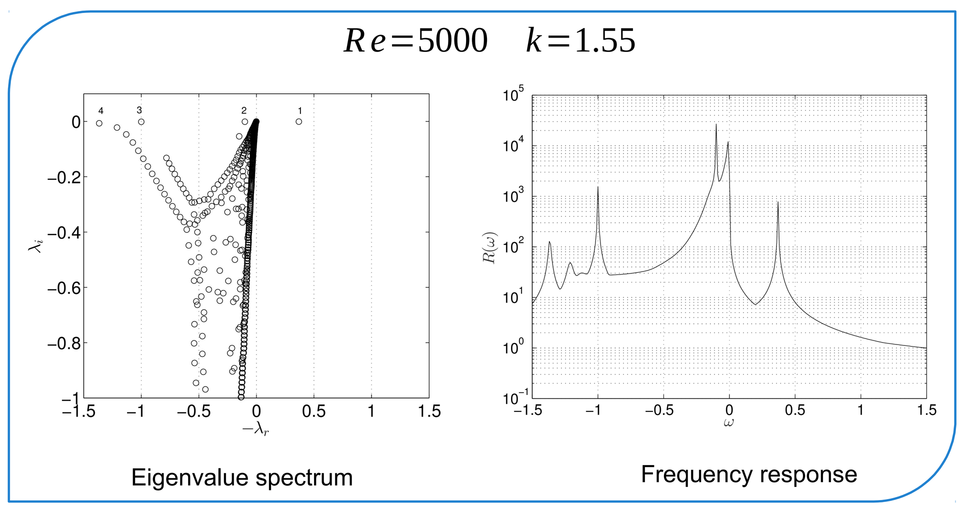

Batchelor vortex $Re=1000$

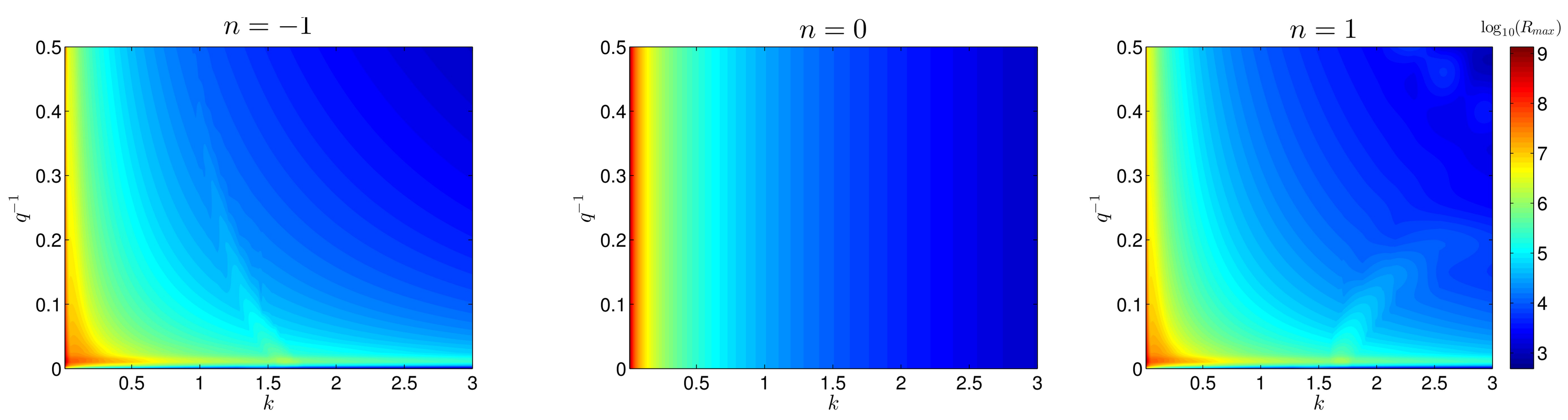

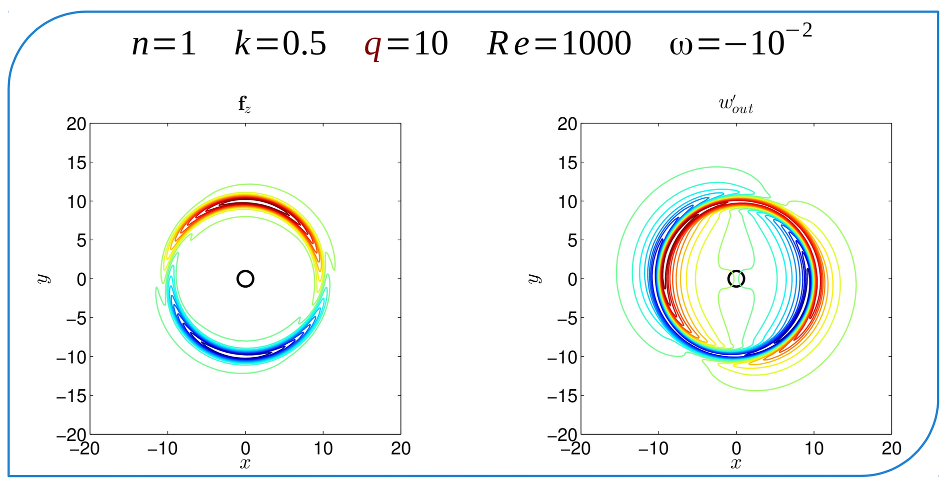

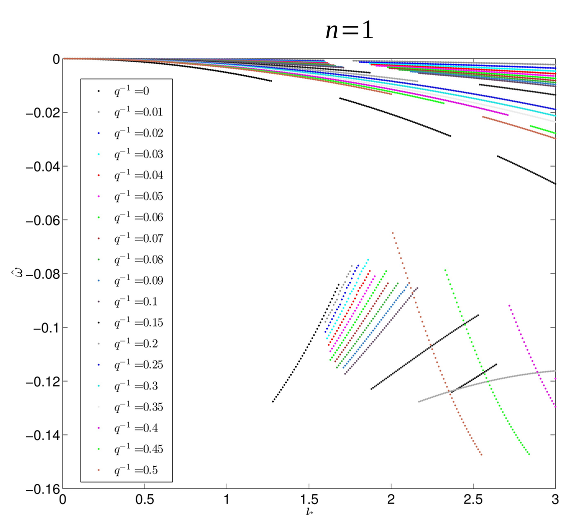

DNS validation

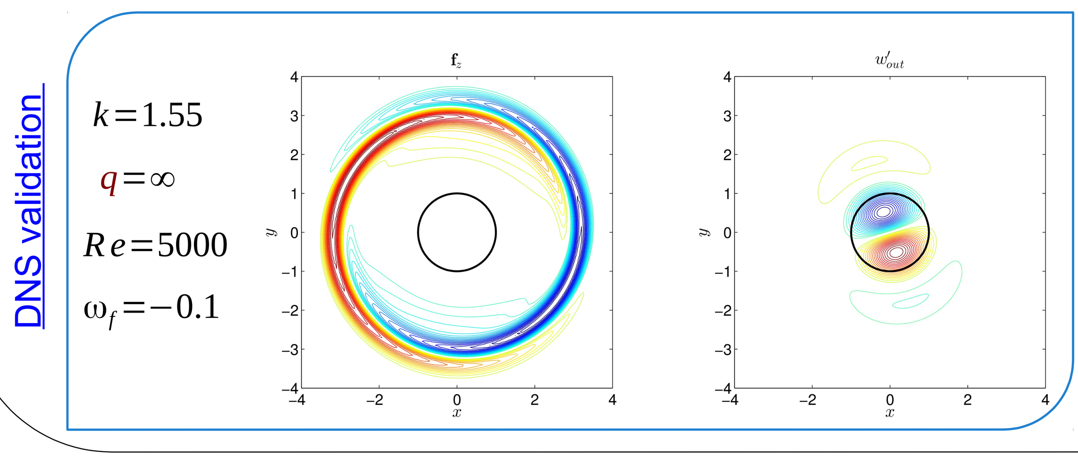

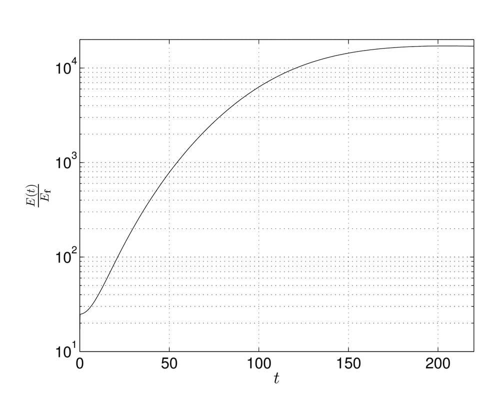

Conclusions and perspectives

- Effect of the axial flow on the optimal response of a Batchelor vortex has been investigated.
  - Lamb-Oseen vortex published results have been recovered.
  - Several integrations parameter paths have been tested.
  - Axisymmetric and helical modes have been simulated for Batchelor vortices:
    - ✓**Axysimmetric**: Maximum gain does not depend on swirl parameter. Stationary optimal forcing.
    - ✓**Helical**: $q-k$ resonant gain maps have been built. Differents branchs for $\hat{\omega}$ have been detected.
  - Optimal forcing structure is so complicated that it is not possible to reproduce experimentally. Understanding the mechanism will provide an insight of where to act.
- Spectral Fourier-based DNS method (Fringe region) validates the theoretical results.

Acknowledgments

This research has been partially funded by *Proyecto de Excelencia de la Junta de Andalucía*, Grant number TEP-P11-7776 and the *Short-Term Postdoctoral Stay* of the Talent Attraction Plan of Andalucía TECH ICE.

Dpto. Ingeniería Mecánica y Mecánica de Fluidos – E.T.S.I. Industriales – Universidad de Málaga and Andalucía Tech
Ampliación de Campus de Teatinos, C/ Doctor Ortíz Ramos, s/n
C.P 29071 Málaga – SPAIN